Journal of Nuclear Materials 386–388 (2009) 257–260

Contents lists available at ScienceDirect

Journal of Nuclear Materials

journal homepage: www.elsevier.com/locate/jnucmat

Mobility of dislocations in thermal aged and irradiated Fe–Cr alloys

D. Terentyev *, G. Bonny, L. Malerba

Structural Materials Group, Institute of Nuclear Materials Science, SCK•CEN, Boeretang 200, B-2400, Mol, Belgium

ARTICLE INFO

PACS:
61.72.Lk
61.82.Bg
61.80.Az
61.72.Qq
62.20.Fe

ABSTRACT

Atomistic simulations are used to study how thermal ageing or radiation-enhanced/induced microstructural changes affect the motion of an edge dislocation in Fe–Cr alloys. Monte Carlo (MC) techniques were used to obtain distributions of Cr atoms in Fe–Cr alloys containing from 5% to 12%Cr, with an *ab initio*-based interatomic potential correctly reproducing the thermodynamic properties of Fe–Cr alloys in the Fe-rich region. The edge dislocation motion was then modelled using molecular dynamics, by applying constant strain-rate and the corresponding flow-stress was monitored, in Fe and Fe–Cr defect-free matrices with random and MC-obtained Cr distributions, as well as in matrices containing Cr precipitates of different sizes and radiation defects (voids and dislocation loops). We show that the flow-stress in concentrated Fe–Cr alloys is much higher than in dilute ones. The presence of Cr precipitates significantly contributes to hardening and their strength increases linearly with size. The critical stress to shear voids and Cr precipitates is higher in Fe–Cr than in pure Fe.

1. Introduction

The choice of 9%Cr ferritic/martensitic steels as structural materials for fusion applications is largely based on the observed minimum radiation-induced embrittlement [1]. Embrittlement in steels with $C_{Cr} > 9\%$ is explained in terms of α–α' demixing, leading to formation of Cr-rich coherent precipitates [2]. Why radiation-induced embrittlement increases for steels with <9% Cr remains unclear, but the well-known tendency of Cr to ordering (in this range of concentrations [3]) may play a role in it, although this contention needs to be demonstrated. Experimental evidence accumulated over 30 years and relatively recent results from atomistic modelling reveal that: (i) adding Cr to Fe (up to 15%) influences the microstructure evolution under irradiation, by suppressing void formation and increasing dislocation loop density (e.g. [4]); (ii) the strength of radiation-induced defects is increased by Cr (as shown by comparative isochronal-recovery tensile tests [5]); (iii) Cr has significant affinity for self-interstitial atoms (SIA), but hardly interacts with vacancies, despite being a slightly oversized atom in Fe [6]; (iv) Cr has unexpectedly strong affinity (0.4 eV) for delocalized interstitial configurations ($\langle 1\,1\,1\rangle$crowdion), as first found in molecular dynamics (MD) simulations and then confirmed by density functional theory (DFT) [6]. These facts suggest that dislocation motion and dislocation-obstacle interaction need to be studied separately in Fe and Fe–Cr alloys to reveal the effect of Cr. In this work, by using MD techniques with a recent DFT-based interatomic potential [7], we present preliminary results revealing the effect of Cr on: (i) $\frac{1}{2}[1\,1\,1]\{1\,\bar{1}\,0\}$ edge dislocation (ED) motion in Fe–Cr matrices, with specific Cr distribution, obtained from Monte Carlo (MC) simulations; (ii) interaction of ED with voids, $\frac{1}{2}[1\,\bar{1}\,1]$ dislocation loops and Cr precipitates.

2. Computational details

The simulations were performed with a many-body potential for Fe–Cr that provides a satisfactory description of phase stability and point-defect/solute interaction [6,7]. ED motion was studied in Fe–xCr body-centered cubic (bcc) solid solutions with $x = 0.5$, 1, 5, 10 and 12%. Alloys with random (Fe–$x\mathrm{Cr}_{\mathrm{RANDOM}}$) and ordered (Fe–$x\mathrm{Cr}_{\mathrm{SRO}}$) Cr distributions were studied, the latter corresponding to thermodynamic equilibrium. In dilute alloys ($\leqslant$1%Cr), consistency with thermodynamics was ensured by simply preventing the presence of Cr–Cr 1st nearest neighbour (nn) pairs. In other alloys the Cr distribution was obtained by exchange MC techniques, as in [8]. In Fe-12%Cr crystals, nearly spherical Cr-rich precipitates ($x > 95\%$) of different diameters ($D_P = 0.6 \div 3.5$ nm) formed in MC simulations at 700 K [8] and were, subsequently used to study precipitate-ED interaction. Conversely, Fe-5%Cr samples showed partial Cr ordering (with a short-range-order parameter of -0.05) after MC simulations at 700 K, correspondingly used to study the effect of ordering on ED motion. In Fe-10%Cr, no significant Cr rearrangement is expected, so only random Cr distributions were considered.

ED motion under load at constant strain-rate ($\gamma = 10^5$ ps^{-1}) was simulated in Fe–Cr crystals, varying Cr content and distribution (as above-described), using a model from [9], to obtain stress–strain

* Corresponding author. Tel.: +32 14 333197; fax: +32 14 321216.
E-mail address: dterenty@sckcen.be (D. Terentyev).

0022-3115/$ - see front matter © 2008 Elsevier B.V. All rights reserved.
doi:10.1016/j.jnucmat.2008.12.106

Table 1
Parameters used in MD simulations of ED motion: *A* – motion in defect-free crystals; *B* – interaction with precipitates having D_P = 0.6 and 1.1 nm; *C* – interaction with precipitates having D_P = 1.7 ÷ 3.5 nm; *D* – interaction with voids and ½[1 $\bar{1}$ 1] SIA loops in Fe-10%Cr and pure Fe matrices. (*L* is the box length in a specified direction).

Parameters/MD simulation	*A*	*B*	*C*	*D*
$L_{\langle 111\rangle}$, nm	35	35	35	35
$L_{\langle 112\rangle}$, nm	28	21	28	21
$L_{\langle 110\rangle}$, nm	8	8	16	12
Number of atoms × 10^3	530	400	1060	550
MD timestep	1 fs for T = 300 K, 2 fs for T = 10 K			
Strain-rate	10^{-5} ps^{-1}			

relationships ($\tau - \gamma$) The interaction of the ED (b = ½[1 1 1]) with voids, ½[1 $\bar{1}$ 1] circular SIA loops and Cr-rich precipitates was studied in Fe and Fe-10%Cr_{RANDOM}. The centre of the precipitate or void lay on the dislocation slip-plane (DSP), while the SIA loop with b = ½[1 $\bar{1}$ 1] (inclined to the DSP) was placed 3 nm below it. In pure Fe, the interaction of the ED with voids and ½⟨1 1 1⟩ loops was already studied in [10–12], including temperature and defect-size effects. Here we have preliminarily performed only simulations in the alloy at 300 K with a void and a loop containing the same number of defects (169), of diameters D_V = 1.6 nm and D_L = 3.3 nm, respectively. The diameter of the precipitate, D_P, was varied to obtain information about critical stress (τ_C) and interaction mechanisms versus size. The MD simulation parameters are summarised in Table 1.

3. Results, discussion and conclusions

Motion of ED in defect-free crystals: The τ–γ relationships for Fe and Fe–Cr crystallites loaded at 10 K are plotted in Fig. 1. In Fe, the τ–γ curve has a saw-like shape, with frequent but regular low peaks. The critical stress for the ED, τ_C (maximum encountered over ~100b), is 25 MPa. In dilute alloys (0.5% and 1%Cr) the peaks are slightly amplified and less regular, due to the weak attractive interaction between ED and Cr (~0.1 eV). In Fe-5,10%Cr_{RANDOM}, the ED glides under significantly higher stress (upper part of Fig. 1). Visualising the ED motion, we observed that in Fe, Fe-0.5 and Fe-1%Cr_{RANDOM}, and in Fe-5%Cr_{SRO}, it moved essentially as a straight line. However, in Fe-5,10%Cr_{RANDOM} it took a waving shape (amplitude ~3 ÷ 6b) and was seen to glide via displacements of individual segments (20 ÷ 60b long), eventually separated by strong pinning obstacles, later identified as small Cr-rich clusters of mainly Cr–Cr 1st nn pairs. The latter exhibit strong repulsive interaction with the core of the ED (0.2 eV). Their presence therefore justifies the remarkable difference in τ–γ curves for Fe-5%Cr alloys, explaining why the ED glides under significantly lower τ_C in Fe-5%Cr_{SRO} than in the random alloy.

Motion of ED in presence of Cr precipitates: The τ–γ relationships for the ED shearing Cr precipitates in Fe-12%Cr alloys at 10 K is shown in Fig. 2(a). The curve obtained in the precipitate-free matrix, is shown, too. As D_P increases, τ_C increases as well. However, for small precipitates ($D_P \leqslant 1.2$ nm) τ_C is comparable to the matrix friction stress. The following interaction mechanism was revealed by visualisation: (i) initially, the ED was repelled by the precipitate; (ii) under increasing τ, it bowed around the precipitate and (iii) finally cut it, so τ_C was reached just before the ED entered the precipitate. The estimated break-away angles were >0 for all precipitate sizes and ED-line lengths (21 and 30 nm) considered here. τ_C vs D_P estimated in Fe and Fe-12%Cr is plotted in Fig. 2(b), which shows linear growth of τ_C (if D_P > 1.5 nm). Note that $\Delta\tau_C$ in Fe and Fe-12%Cr is constant and about equal to τ_C in the precipitate-free Fe–Cr matrix, suggesting that τ_C increases in the alloys due to the higher friction stress.

Motion of ED in presence of a void or a loop: The interaction of the ED (b = 1/2[1 1 1]) with a ½[1 $\bar{1}$ 1] SIA loops may result in complete or partial loop absorption, depending on D_L and temperature, as in pure Fe [11,12]. Reactions with 169-SIA loops in Fe were already reported [12], using the same potential as here. At 300 K, complete loop absorption by the ED was observed, in three steps [12]: (i) formation of a common [0 $\bar{1}$ 0] segment; (ii) emission of a screw dipole; (iii) propagation of the [0 $\bar{1}$ 0] pinning segment across

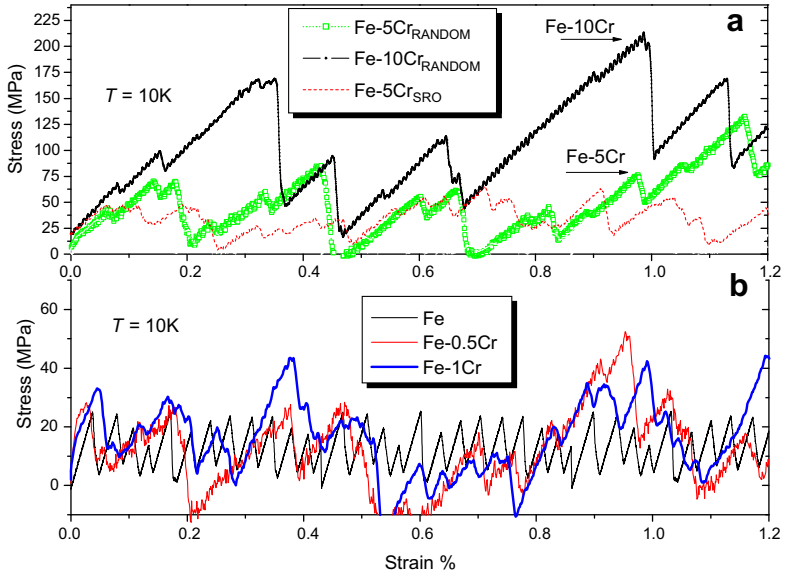

Fig. 1. Stress–strain curves obtained in MD simulations at 10 K of ED motion in Fe and Fe–Cr alloys of different Cr content. (a) Concentrated alloys; (b) dilute alloys.

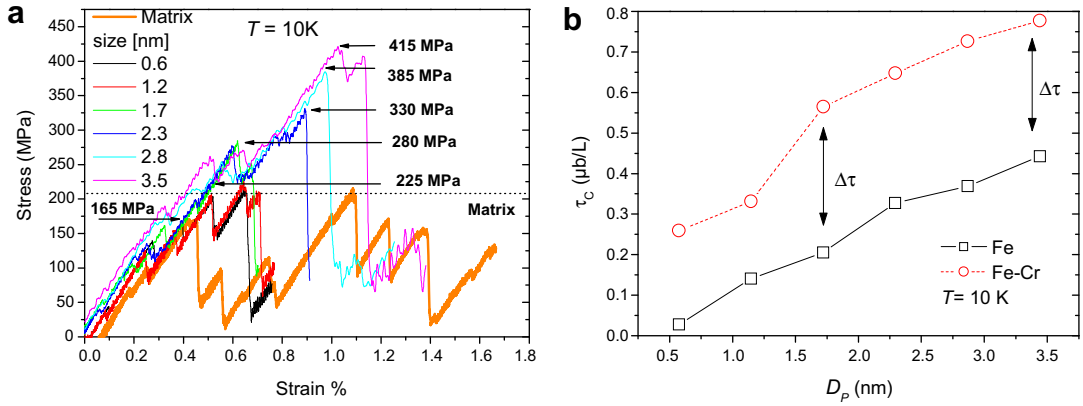

Fig. 2. (a) Stress–strain curves obtained in MD simulations at 10 K modelling motion of ED in Fe-12%Cr alloys containing Cr-rich precipitates of different sizes. (b) Estimated τ_C (in $\mu b/L$ units, $\mu = 70$ GPa) for the ED to cut a Cr-rich precipitate in Fe and Fe-12%Cr alloy vs. precipitate size

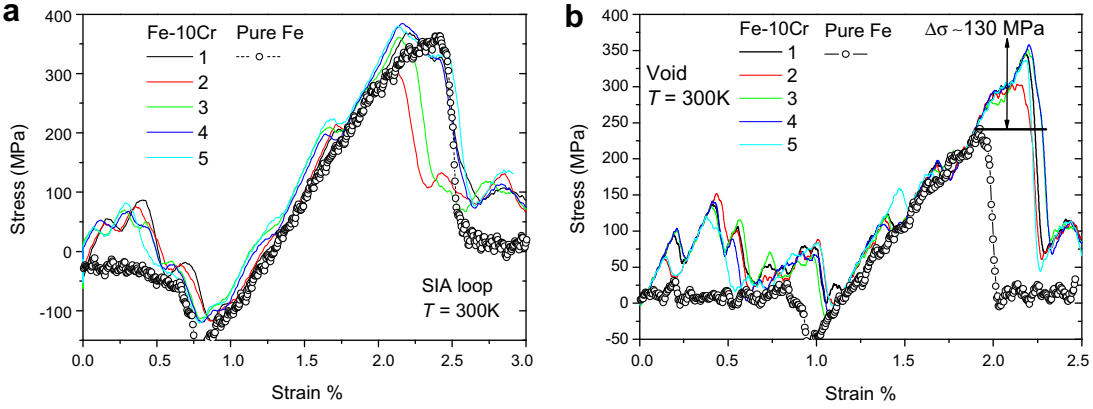

Fig. 3. Stress–strain curves obtained in five MD simulations performed at 10 K in Fe-10%Cr, and one in pure Fe, modelling the interaction of the ED with (a) ½[1 $\bar{1}$ 1] SIA loop and (b) void, each containing 169 defects.

the loop combined with a screw dipole cross-slip (and its annihilation) at τ_C, leading to the incorporation of the loop in the ED as a set of superjogs. Importantly, at step (ii) the ED arms keep moving further, being connected to the pinning [0 $\bar{1}$ 0] segment via the screw dipole, whose length increases constantly until step (iii) occurs. The controlling factor is the mobility of the [0 $\bar{1}$ 0] segment (which is sessile in the DSP). Conversely, when the ED interacts with a void in Fe, the dislocation line bows smoothly (keeping arch-line shape) with increasing τ. The release occurs with the formation of a step in the void surface, accompanied by climb of the ED and absorption of a few vacancies from the void [10].

Reactions of the ED with voids and ½[1 $\bar{1}$ 1] SIA loops (containing 169 defects each) in Fe-10%Cr_{RANDOM} alloys were modelled, too (varying Cr arrangement near defects using five different random seeds). The corresponding τ–γ curves are shown in Fig. 3. The reaction mechanisms in Fe–Cr are the same as in Fe. For the ½[1 $\bar{1}$ 1] loop (Fig. 3(a)), τ_C appears not to vary with Cr (τ_C = 360 MPa), whereas the average τ_C (over five runs) for the void (Fig. 3(b)) increases by 130 MPa in the presence of Cr as compared to pure Fe, where τ_C = 240 MPa. The dislocation line shape, visualised at τ_C, was seen to have significantly larger curvature in Fe–Cr than in Fe, with a consequently higher line-tension. We believe that this effect should be attributed to the additional matrix resistance to the glide of the ED. $\Delta\tau_C$ = 130 MPa between Fe–Cr and Fe for voids is close to $\Delta\tau_C$ = 100 MPa for Cr precipitates, while τ_C for the 169-½[1 $\bar{1}$ 1] SIA loop is the same in Fe and Fe–Cr, which is probably due to insensitivity of short [0 $\bar{1}$ 0] segment mobility to the presence of Cr.

More thorough studies of Cr effects on the behaviour of dislocations in Fe–Cr alloys (i.e. temperature, defect size, interaction geometry etc.) are ongoing. For the moment, the following preliminary conclusions can be drawn:

1. Concentrated random Fe–Cr alloys provide stronger resistance to the ½[1 1 1] {1 $\bar{1}$ 1} ED motion than dilute alloys, because the resistance of Cr–Cr pairs (repelling the ED) is much stronger than that of isolated Cr atoms (weakly attracting the ED); in the absence of close Cr–Cr pairs, ordered alloys provide weaker resistance than random ones.
2. Cr precipitates were observed to be sheared by the ED, rather than by-passed. For precipitates, τ_C grows linearly with size and it is higher in Fe–Cr than in pure Fe, making a difference approximately equal to the friction stress of the same Fe–Cr matrix without precipitate.
3. Reactions of the ED with voids and ½[1 $\bar{1}$ 1] SIA loops proceed via the same mechanisms as in Fe. However, τ_C to cut the void is higher in Fe–Cr than in Fe.

Acknowledgements

The support by the European Commission is acknowledged, under the Underlying Technology part of the European Fusion Programme.

References

[1] A. Kohyama, A. Hishinuma, D.S. Gelles, R.L. Klueh, W. Dietz, K. Ehrlich, J. Nucl. Mater. 233–237 (1996) 138.
[2] P. Dubuisson, D. Gilbon, J.L. Séran, J. Nucl. Mater. 205 (1993) 178.
[3] I. Mirebeau, M. Hennion, G. Parette, Phys. Rev. Lett. 53 (1984) 687.
[4] E.A. Little, D.A. Stow, J. Nucl. Mater. 87 (1979) 25;
N. Yoshida, A. Yamaguchi, T. Muroga, Y. Miyamoto, K. Kitajima, J. Nucl. Mater. 155–157 (1988) 1232.
[5] K. Suganuma, H. Kayano, J. Nucl. Mater. 118 (1983) 234.
[6] D. Terentyev, L. Malerba, A.V. Barashev, Philos. Mag. Lett. 85 (2005) 587;
D. Terentyev, P. Olsson, L. Malerba, A.V. Barashev, J. Nucl. Mater. 362 (2007) 167;
D. Terentyev, P. Olsson, T.C.P. Klaver, L. Malerba, Comp. Mat. Sci. 43 (2008) 1183.
[7] P. Olsson, J. Wallenius, C. Domain, K. Nordlund, L. Malerba, Phys. Rev. B 72 (2005) 214119.
[8] G. Bonny, D. Terentyev, L. Malerba, Comp. Mat. Sci. 42 (2007) 107.
[9] Yu.N. Osetsky, D.J. Bacon, Model. Simul. Mater. Sci. Eng. 11 (2003) 427.
[10] D.J. Bacon, Yu.N. Osetsky, Mat. Sci. Eng. A 400&401 (2005) 353.
[11] D.J. Bacon, Yu.N. Osetsky, Z. Rong, Philos. Mag. 86 (2006) 3921.
[12] D. Terentyev, L. Malerba, D.J. Bacon, Yu.N. Osetsky, J. Phys. Condens. Matter 19 (2007) 456211.